Progress In Electromagnetics Research C, Vol. 70, 43–51, 2016

A Compact Low-Profile and Quad-Band Antenna with Three Different Shaped Slots

Wei Xue, Mi Xiao*, Guoliang Sun, and Fang Xu

Abstract—A compact quad-band slot antenna is presented in this paper. The proposed antenna consists of ground plane, dielectric material and top radiation patch. Firstly, symmetrical L-shaped slots are inserted in a radiation patch. Then to achieve multiband performances, symmetrical square spiral slots and a snakelike area with two symmetrical arms enclosed by a long slot in the ground plane are adopted. The process of design and parametric studies are illustrated in detail. The final quad-band antenna has a small size of $0.22\lambda_g \times 0.28\lambda_g = 17 \times 22\,\text{mm}^2$ (where λ_g is the guide wavelength) and covers the frequency bands from 2.39 to 2.48 GHz for lower WLAN, 3.64–3.73 GHz for downlink and 5.98–6.30 GHz for uplink standard satellite communications, and 6.97–7.18 GHz mainly used by the Indian National Satellite System (INSAT). The measured results of the proposed quad-band antenna are in accordance with simulated analysis and show good performance of return loss characteristics, radiation patterns, bandwidths and gains. Especially, with a very small size, the proposed antenna is suitable to be integrated with a portable device for varieties of wireless communication applications.

1. INTRODUCTION

With the rapid development of wireless communication, many related standards appeared for different applications such as worldwide interoperability for microwave access (WiMAX), WLAN, and satellite communications. Demands for the multiband antenna have increased very fast to support these standards on a single wireless device. Moreover, with the prevalence of mobile devices, it is increasingly significant and necessary to propose more compact antennas comparable with the small size of these portable equipments. For this reason, a microstrip printed antenna is more suitable than any other types of antennas as it is easier to achieve multiband characteristics with the features of miniaturization, low profile, light weight and easy processing [1].

In the past years, some printed microstrip multiband antennas [1–12] have been designed. In [2], a compact quad-band microstrip antenna with two rectangular notches on the radiation patch is proposed and analysed for S-band and C-band applications. In [3], a triple-band antenna for mobile applications is proposed by four-step selecting appropriate angles and number of the hook-shaped strips on the radiation patch. In [4], triple-band characteristics for WiMAX/WLAN applications is achieved by using a structure composed of three simple circular-arc-shaped strips, whose whole geometry looks like "ear" type. Unlike above antennas which achieve multiband characteristics by changing the geometry of the radiation patch, some other authors prefer to insert additional slots in the antennas. For example, a band-notched UWB microstrip antenna is proposed with an S-shaped slot in the radiation patch and a pair of symmetrical C-shaped slots on the ground plane [5]. In [7], a circular patch antenna based on six open elliptical-ring slots on the radiation patch and shorting vias with conical radiation patterns is proposed. A coplanar waveguide (CPW)-fed planar monopole antenna with triple-band operation for WiMAX and WLAN applications is presented [9], where two bent slots with different sizes on

Received 27 October 2016, Accepted 22 November 2016, Scheduled 7 December 2016
* Corresponding author:Mi Xiao (xiaomi@tju.edu.cn).
The authors are with the School of Electronic Information Engineering, Tianjin University, Tianjin 300072, China.

the radiation patch are employed. In [10], a coupled dual-U-shaped antenna for WiMAX triple-band operation is presented. Three operating frequency bands for GPS/WiMAX/WLAN are achieved by a pair of L-shaped slots and rectangular slots, and defected ground structure in [11]. And in [12], by using two pairs of eye-shaped slots, the authors reduce the side lobe levels of the radiation pattern of their proposed printed antenna.

All the above antennas perform well at achieving multiband characteristics, nevertheless, they tend to have larger sizes, such as the one with a size of $30 \times 30 \times 1.6\,\text{mm}^3$ in [2], authors only provided two simple rectangular notches on the radiation patch without introducing any slots. In [4], the antenna has a total size of $18 \times 37 \times 1\,\text{mm}^3$, on account of metal patches occupying more space. And in [6], the presented quad-band antenna has a size of $15.5 \times 16.4 \times 1.56\,\text{mm}^3$ for the patch, but need an additional height of 6 mm between its patch and ground plane.

In this paper, a compact quad-band antenna with three shaped slots for the applications of WLAN and C-band satellite communications is designed based on theoretical parametric studies and experiments. Different from most existing similar antennas which exploit only one type of slots, maybe through tuning the position and number of them, we introduce three different structures of slots for achieving better performance on small size and quad-band characteristics. The proposed quad-band antenna has a small size of $0.22\lambda_g \times 0.28\lambda_g = 17 \times 22\,\text{mm}^2$ (where λ_g is the guide wavelength) with operating bands covering various applications, such as 2.4 GHz WLAN, 3.7/6 GHz for standard satellite communications and 7 GHz mainly used by INSAT. And the simulated results obtained by HFSS agree well with the measured results.

2. ANTENNA DESIGN AND PARAMETRIC STUDY

The antenna is designed on a rectangular FR4 substrate with $\varepsilon_r = 4.4$ and loss tangent of 0.02. Its geometry and photograph are shown in Fig. 1.

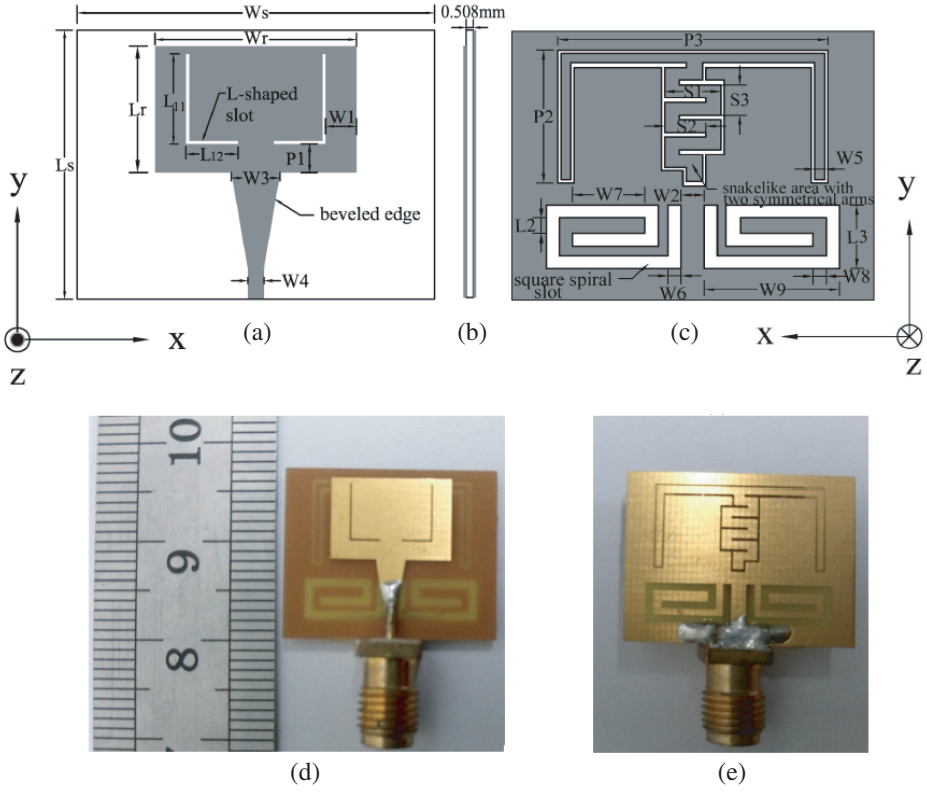

Figure 1. Geometry of the proposed antenna: (a) top view, (b) side view and (c) bottom view; Photograph of the proposed antenna, (d) top view and (e) bottom view.

To reduce the size of the antenna while keeping the desired properties, slots are inserted in both the radiation patch and ground plane. These slots change the current flows, so that multiband characteristics can be achieved. The length of the slot L_{total} is set close to a quarter of the guided wavelength λ_g, which can be calculated from the following equation:

$$\lambda_g = \frac{c}{f\sqrt{\varepsilon_{reff}}} \tag{1}$$

where c is the speed of light, f the desired resonant frequency and ε_{reff} the effective permittivity computed by the formula:

$$\varepsilon_{reff} = \frac{\varepsilon_r + 1}{2} \tag{2}$$

The final optimized parameters of the proposed antenna are presented in Table 1. And the design steps are presented in Fig. 2 and illustrated in detail as follows.

Table 1. Parameters of the proposed antenna (mm).

Ws	Ls	hs	Wr	Lr	L_{11}	L_{12}	L2	L3	W1	W2	W3
22	17	0.508	12.4	8	5.7	2.8	1	4	1.9	1.4	3
W4	W5	W6	W7	W8	W9	P1	P2	P3	S1	S2	S3
1	0.6	0.8	4.4	0.8	8.2	2	8.4	16.4	3.4	2.5	1.9

2.1. Single-Band Antenna Structure

The single-band antenna consists of a ground plane and a rectangular radiation patch with two symmetrical L-shaped slots. To excite the antenna, a 50-Ω microstrip feed line with a width of W4 is used, and the beveled edge is introduced for better performance as shown in Fig. 2(a). Fig. 3(a) indicates that inserting the L-shaped slots introduces a resonant frequency. For the acquired resonant frequency at about 7.4 GHz shown in Fig. 3, $L_{total} = L_{11} + L_{12} = 8.5$ mm, which is close to $\frac{\lambda_g}{4} = \frac{c}{4f\sqrt{\varepsilon_{reff}}} = 6.2$ mm. Furthermore, the microstrip with the introduced beveled edge, which is a resistance gradually changing structure, improves the return loss characteristics and achieves impedance matching at the desired resonant frequency, as shown in Figs. 3(a) and (b), respectively.

Figure 2. Process of designing the proposed antenna.

Parametric studies for L_{11}, L_{12}, P1 and W1 are carried out, and the results of return loss characteristics are presented in Figs. 3(c)–(e), which indicate that the desired resonant frequency decreases as W1 increases. We can also see that when P1 is much larger or smaller, the L-shaped slots will not work well. The optimal L_{11} and L_{12} are set to 5.7 and 2.8 mm, respectively.

2.2. Dual-Band Antenna Structure

By inserting slots in the ground plane and carefully adjusting their parameters, additional resonances can be excited [10]. Considering making good use of the space, two symmetrical square spiral slots are

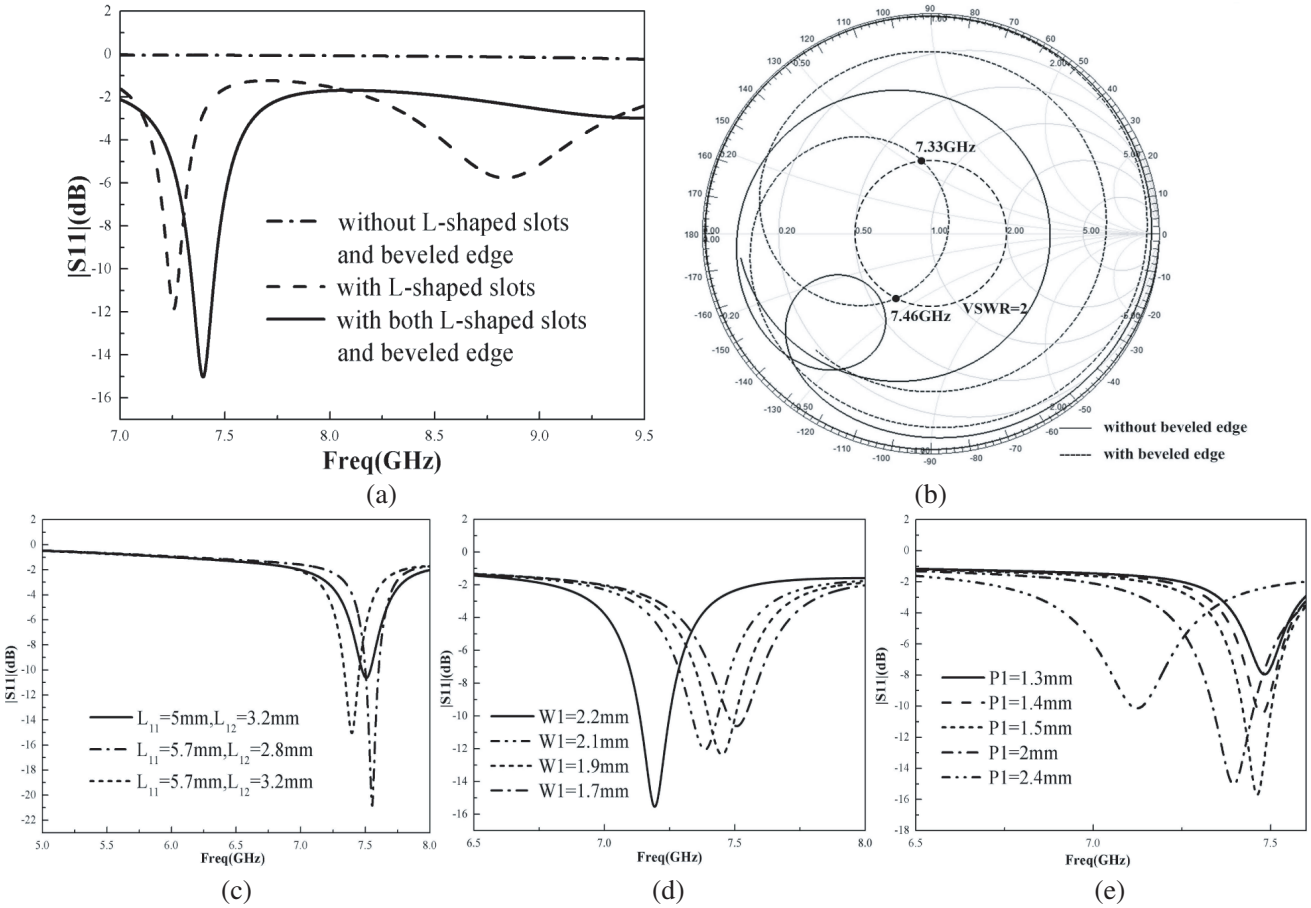

Figure 3. Simulated return loss characteristics of the single-band antenna (a) with only radiation patch, L-shaped slots, and both the L-shaped slots and beveled edge and (b) its impedance matching condition (L_{11} = 5.7 mm, L_{12} = 2.8 mm, W1 = 1.9 mm and P1 = 2 mm), and for (c) different L_{11} and L_{12}, (d) different W1 and (e) different P1.

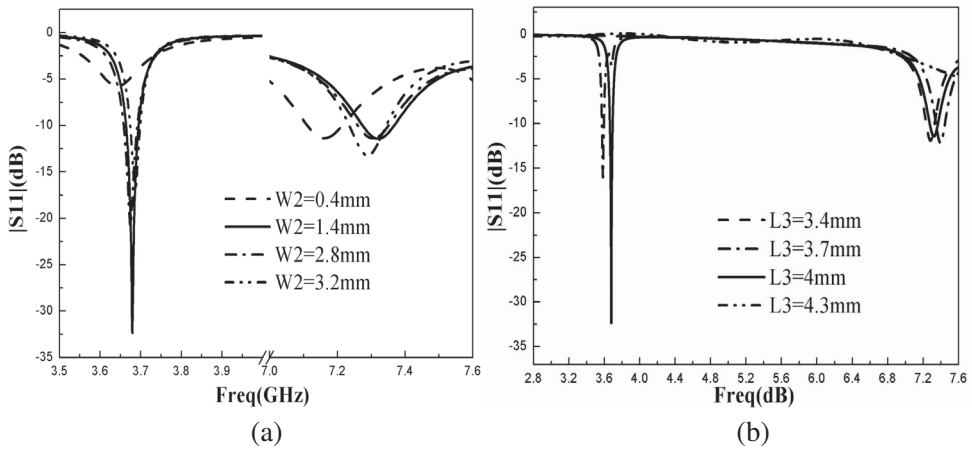

Figure 4. Simulated return loss characteristics of the dual-band antenna for (a) different W2 and (b) different L3.

embedded on the lower edge of the ground plane as shown in Fig. 2(b). They can be efficiently excited when being placed near the microstrip feed line and along with the current flow.

As shown in Fig. 4, the slots bring in a desired resonant frequency at about 3.7 GHz for downlink frequency of standard satellite communications. The electrical length is appropriately equal to the total length of the current path within the square spiral slot, i.e., $L_{total} = L3 - 2 \times W6 + 2 \times W7 + 2 \times W8 = 12.8\,mm$, which is close to $\frac{\lambda_g}{4} = 12.3\,mm$. We can observe that the distance W2 should be large enough to reduce the coupling between two slots, whereas a too large W2 will weaken the exciting degree at desired resonant frequency. The optimal distance is set to 1.4 mm. Similarly, the exciting degree at 3.7 GHz is weakened when L3 is small, and larger L3 increases the coupling with other structures. The optimized L3 is 4 mm. It is also noted that varied parameters have no significant effects on the return loss characteristics of previous resonant frequency at about 7.4 GHz.

2.3. Quad-Band Antenna Structure

The resonant frequencies for lower WLAN at about 2.4 GHz and uplink frequency of standard satellite communications at about 6 GHz can be attained by segmenting out a snakelike area with symmetrical arms enclosed by a long slot, which is based on the common U-shaped arms, and can produce longer current path in small area. For the new introduced structure shown in Fig. 2(c), most widths of the

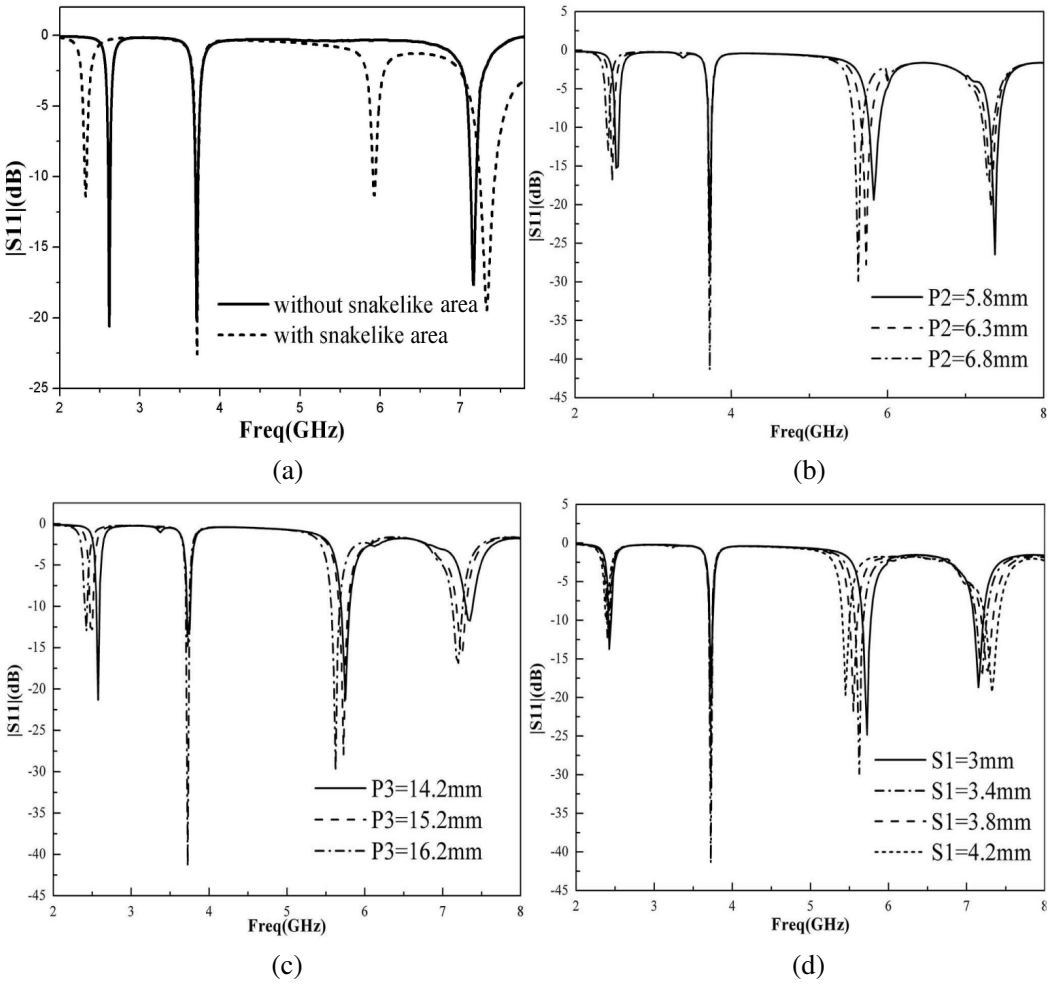

Figure 5. Simulated return loss characteristics of the quad-band antenna (a) with and without the snakelike area (P2 = 8.4 mm, P3 = 16.4 mm and S1 = 3.4 mm), and for (b) different P2, (c) different P3 and (d) different S1.

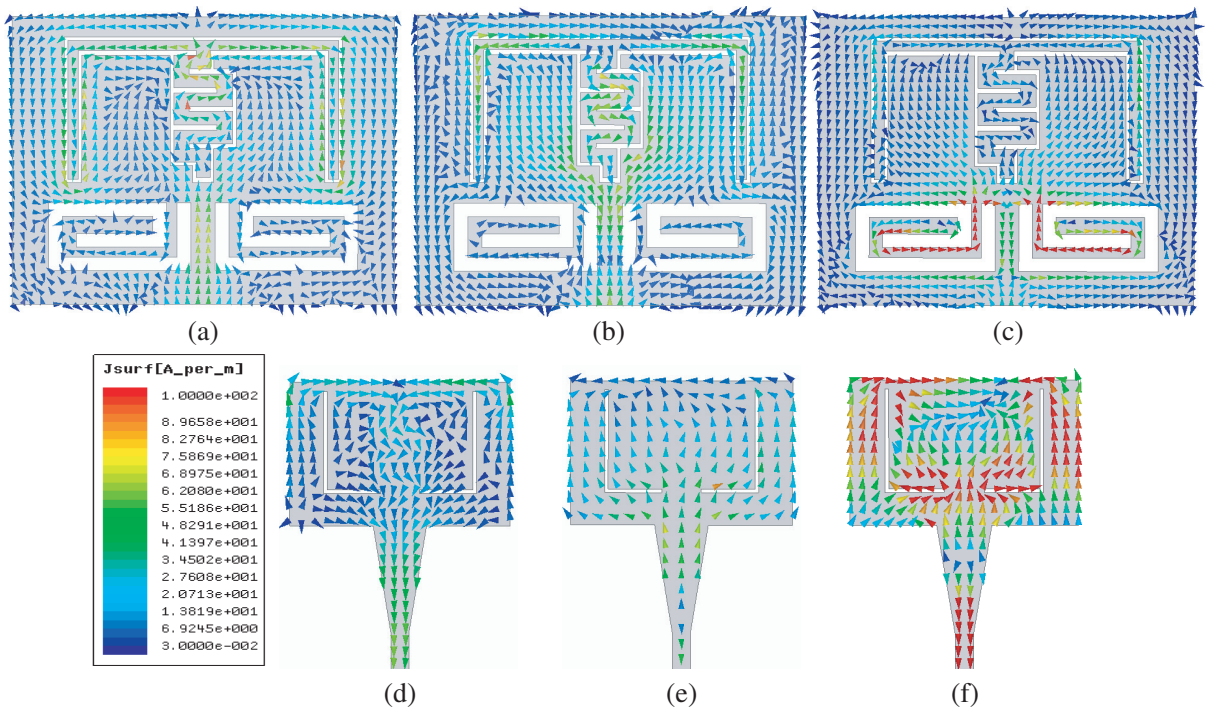

Figure 6. Current distribution of the proposed quad-band antenna at (a) 2.4 GHz (bottom view), (b) 6 GHz (bottom view), (c) 3.7 GHz, (d) 2.4 GHz (top view), (e) 6 GHz (top view) and (f) 7.4 GHz.

slot are set to 0.2 mm, while the horizontal lines near the snakelike area are set to 0.3 mm. Fig. 5(a) indicates that the resonant frequency at about 2.6 GHz can be excited when only using the U-shaped symmetrical arms. After adding the additional snakelike area, the other resonant frequency at 6 GHz is excited.

For detailed discussions, the simulated current distribution is shown in Fig. 6. The current path for 2.6 GHz does not change main direction compared with the common U-shaped arms except that the resonant frequency decreases slightly to 2.4 GHz because the current path becomes longer than before as shown in Figs. 6(a) and (d), whereas for the second resonant frequency at about 6 GHz, the current changes direction as shown in Figs. 6(b) and (e). In this case, the direction of the coupling between the radiation patch and the snakelike area with symmetrical arms is changed, so two resonant modes can be excited [13]. According to the current distribution in the symmetrical U-shaped arms, the electrical length of 2.4 GHz is about $\frac{\mathrm{P3}}{2} + \mathrm{P2} = 16.6\,\mathrm{mm}$, where $\frac{\lambda_g}{4} = 19.0\,\mathrm{mm}$. Similarly, for 6 GHz achieved by the snakelike area, $\mathrm{L}_{total} \approx 2 \times \mathrm{S2} + 2 \times \mathrm{S3} = 8.8\,\mathrm{mm}$, and $\frac{\lambda_g}{4} = 7.6\,\mathrm{mm}$. And the current distribution on this proposed quad-band antenna at two previous resonant frequencies 3.7 and 7.4 GHz are shown in Figs. 6(c) and (f), respectively. It is clearly seen that the current is concentrated near corresponding slots.

Figures 5(b)–(d) show the influence on return loss characteristics of a quad-band antenna when P2, P3 or S1 varies. It is observed that the small changes in the lengths of P2 and P3 have significant influence on the resonant frequencies at 2.4 GHz and 6 GHz, and increasing P2 or P3 achieves better performance. Selected S1 = 3.4 mm achieves the best return loss characteristics among others, especially at about 6 GHz.

3. SIMULATED AND MEASURED RESULTS

In Fig. 7(a), the measured and simulated return loss characteristics of the quad-band antenna are presented. It is observed that the measured and simulated results are consistent at lower frequencies 2.4 and 3.7 GHz. And at higher frequencies 6 and 7 GHz, the simulated result with the SMA connector

appears more close to the measured result than the simulated result without SMA. This may be because higher frequencies are more sensitive to machining precision and the effects of specific connectors whose sizes are comparable with the antenna. The measured radiation patterns of the quad-band antenna are displayed in Fig. 8. It can be seen that the proposed antenna provides directional radiation patterns, which is suitable since it is mainly applied to satellite communications.

Measured gains in each band are shown in Fig. 7(b). The gains were measured at far field using substitution method, where two horn antennas whose gains had been known were employed to compute the gains of our antenna. Firstly, our proposed antenna was placed on a suitable position to be tested, and then it was replaced with the second calibrated horn antenna with known gain and was measured in a similar way. Difference between these two repeatedly measured signal powers will be used to calculate the final gain. We can see the gains generally become higher as the frequencies increase, because the limitation of the small size to higher frequencies is alleviated since the higher frequency means shorter wavelength. The comparison results with other works in Table 2 indicate that our antenna is the most compact both in terms of size and electrical dimension. Moreover, our antenna can not only be applied to the low-frequency applications, such as WLAN, but also cover the higher C-band frequencies used for satellite communications with acceptable bandwidth performance.

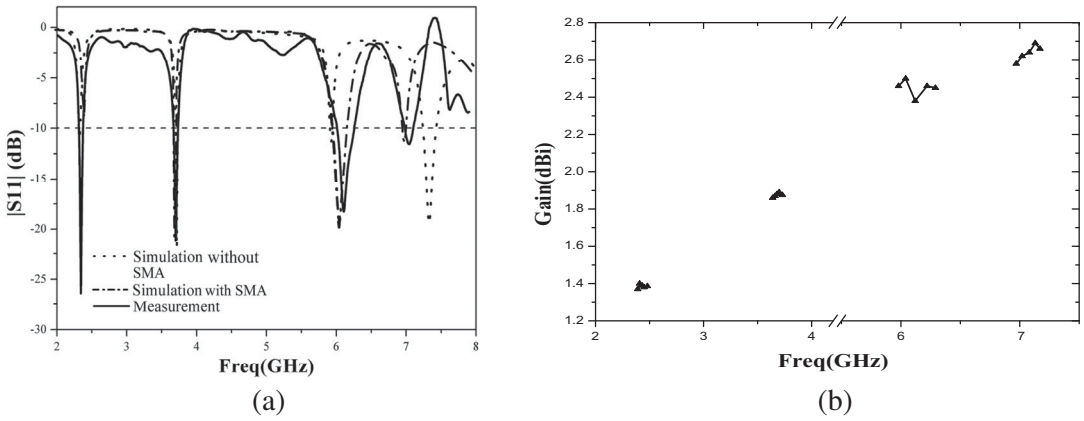

Figure 7. (a) |S11| and (b) measured gains of the proposed quad-band antenna.

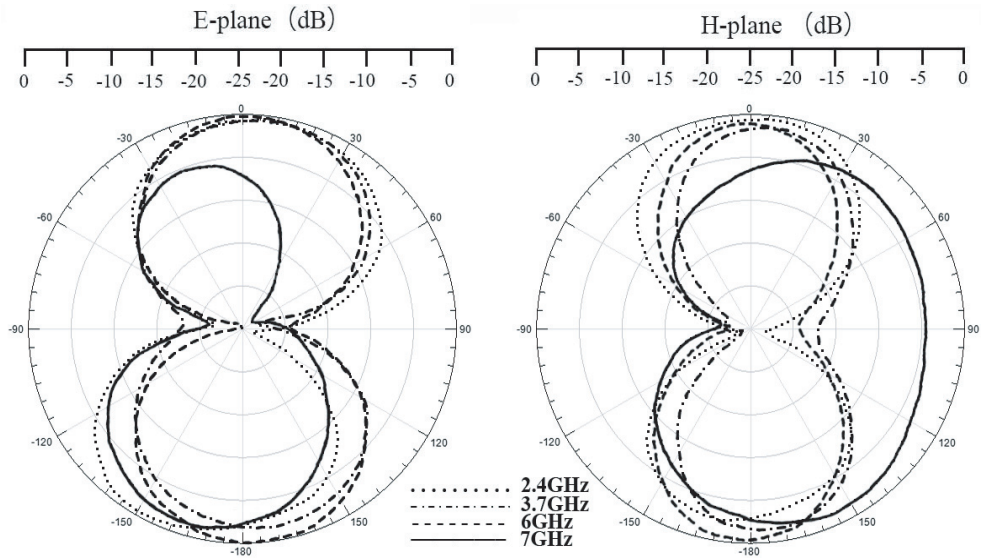

Figure 8. Measured radiation patterns of the proposed quad-band antenna.

Table 2. Comparisons with other works.

Ref.	No. of bands	Electrical dimensions ($\lambda_g{}^2$)	sizes (mm^2)	Resonant frequencies (GHz)	Bandwidths (MHz)
[2]	Quad-band	0.77×0.77	30×30	(1) 4.7 (2) 5.14 (3) 5.7 (4) 6.3	(1) 100 (2) 170 (3) 120 (4) 130
[4]	Triple-band	0.21×0.43	18×37	(1) 2.5 (2) 3.5 (3) 5.5	(1) 400 (2) 480 (3) 1000
[7]	Triple-band	0.50×0.50	47×47	(1) 2.4 (2) 3.5 (3) 5.8	(1) 90 (2) 200 (3) 1000
[8]	Triple-band	0.37×0.41	30×34	(1) 2.5 (2) 3.5 (3) 5.2	1) 320 2) 600 3) 830
The proposed	Quad-band	0.22×0.28	17×22	(1) 2.4 (2) 3.7 (3) 6 (4) 7	(1) 90 (2) 90 (3) 320 (4) 210

4. CONCLUSION

In this paper, a very compact slot quad-band antenna is proposed through a three-step design, where parameter tuning methods to the position and size of three different structures and related theoretical analysis are presented for each step. Finally, four resonant frequencies at about 2.4, 3.7, 6 and 7 GHz for several practical applications can be obtained. Especially, with a novel snakelike area and a square spiral slot, the patch size is reduced to $17 \times 22\,mm^3$ ($0.22\lambda_g \times 0.28\lambda_g$). Due to such a small size, the proposed antenna is applicable to portable application. In addition, our antenna achieves a large range of available resonant frequencies from about 2.4 to 7 GHz, making it suitable in various scenes.

REFERENCES

1. Chu, Q. X. and L. H. Ye, "Design of compact dual-wideband antenna with assembled monopoles," *IEEE Transactions on Antennas and Propagation*, Vol. 58, No. 12, 4063–4066, 2011.
2. Singh, V., B. Mishra, and P. N. Tripathi, "A compact quad-band microstrip antenna for s and c-band applications," *Microwave and Optical Technology Letters*, Vol. 58, No. 6, 1365–1369, 2016.
3. Naser-Moghadasi, M., R. A. Sadeghzadeh, M. Fakheri, T. Aribi, T. Sedghi, and B. S. Virdee, "Miniature hook-shaped multiband antenna for mobile applications," *IEEE Antennas and Wireless Propagation Letters*, Vol. 11, No. 12, 1069–1099, 2012.
4. Zhai, H., Z. Ma, Y. Han, and C. Liang, "A compact printed antenna for triple-band WLAN/WiMAX applications," *IEEE Antennas and Wireless Propagation Letters*, Vol. 12, No. 1921, 65–68, 2013.
5. Ojaroudi, N., M. Ojaroudi, and H. Ebarhimian, "Band-notched UWB microstrip slot antenna with enhanced bandwidth by using a pair of C-shaped slots," *Microwave and Optical Technology Letters*, Vol. 54, No. 2, 515–518, 2012.
6. Singh, D. K., B. K. Kanaujia, S. Dwari, G. P. Pandey, and S. Kumar, "Novel quad-band circularly polarized capacitive-fed microstrip antenna for C-band applications," *Microwave and Optical Technology Letters*, Vol. 57, No. 11, 2622–2628, 2015.
7. Chen, W. F., D. Yu, and S. X. Gong, "An omnidirectional triple-band circular patch antenna based on open elliptical-ring slots and the shorting vias," *Progress In Electromagnetics Research*, Vol. 150, 197–203, 2015.

8. Basaran, S. C., U. Olgun, and K. Sertel, "Multiband monopole antenna with complementary split-ring resonators for WLAN and WiMAX applications," *Electronics Letters*, Vol. 49, No. 10, 636–638, 2013.
9. Liu, H. W., C. H. Ku, and C. F. Yang, "Novel CPW-fed planar monopole antenna for WiMAX/WLAN applications," *IEEE Antennas and Wireless Propagation Letters*, Vol. 9, No. 1, 240–243, 2010.
10. Koo, T. W., D. Kim, J. I. Ryu, J. C. Kim, and J. G. Yook, "A coupled dual-U-shaped monopole antenna for WiMAX triple-band operation," *Microwave and Optical Technology Letters*, Vol. 53, No. 53, 745–748, 2011.
11. Chen, S., M. Fang, D. Dong, M. Han, and G. Liu, "Compact multiband antenna for GPS/WiMAX/WLAN applications," *Microwave and Optical Technology Letters*, Vol. 57, No. 8, 1769–1773, 2015.
12. Ma, K., Z. Zhao, J. Wu, M. S. Ellis, and Z. P. Nie, "A printed Vivaldi antenna with improved radiation patterns by using two pairs of eye-shaped slots for UWB applications," *Progress In Electromagnetics Research*, Vol. 148, No. 148, 63–71, 2014.
13. Zaker, R., C. Ghobadi, and J. Nourinia, "Bandwidth enhancement of novel compact single and dual band-notched printed monopole antenna with a pair of L-shaped slots," *IEEE Transactions on Antennas and Propagation*, Vol. 57, No. 12, 3978–3983, 2009.